Photon Netw Commun (2017) 34:461–467
DOI 10.1007/s11107-017-0704-1

ORIGINAL PAPER

A high-speed phosphorescent LED-based visible light communication system utilizing SQGNRC precoding technique

Hai-Chao Guo[1,2,3] · Yin-Fan Xu[2] · Xiao-Jun Li[3] · Li Zhang[3] · Yan-Jin Wang[2] · Nan Chi[2]

Received: 2 February 2016 / Accepted: 21 April 2017 / Published online: 12 May 2017

Abstract Peak-over-average power ratio (PAPR) control utilizing precoding technique based on square root-generalized raised cosine function is proposed and verified experimentally through a visible light communication system employing phosphor-based white light-emitting diodes for the first time. The simulation results show that the improved precoding matrix can further reduce PAPR by nearly 1 dB compared with existing precoding matrix based on square root raised cosine function and significantly achieve 3.5 dB improvement in contrast to original signals without precoding. The experimental result also proves that the bit error rate performance can be effectively improved by 1.62 dB at the same bandwidth and 0.76 dB at the same raw data rate in terms of quality factor when proposed precoding technique is applied, which clearly demonstrates its benefit and feasibility.

Keywords Visible light communication · Light-emitting diodes · Peak-to-average power ratio · Precoding

1 Introduction

Visible light communication (VLC) based on light-emitting diodes (LED) has been widely recognized as a promising technology considering its advantages such as being cost effective, license free, immune to electromagnetic interference, and highly secure. Compared with red–green–blue (RGB) LED, phosphor-based white LED is more cost-efficient due to its simple technological design and thus more suitable for practical application. In order to improve the spectral efficiency in VLC system, orthogonal frequency-division multiplexing (OFDM) has been widely implemented [1]. However, high peak-over-average power ratio (PAPR) has been widely cited as one of the drawbacks of OFDM modulation [2,3].

In the wireless OFDM case, there are a number of PAPR problems, including multiple-input/multiple-output (MIMO) multiplication due to simultaneously control of parallel transmit signals particularly when considering a huge number of transmit antennas, and multiuser systems put additional side constraints on the parallel transmit signals which are difficult to implement on top of conventional approaches [4]. In VLC context, an optimal OFDM signal power used to modulate the LED intensity is required in order to control the LED nonlinearity induced distortion. However, PAPR will not only degrade the performance of linear power amplifier but also introduce high nonlinear effect. In this case, PAPR reduction techniques are considered to reduce power back off levels [5].

Till now, a series of solutions to the PAPR problem have been proposed to achieve PAPR reduction at the expense of transmit signal power increase, bit error rate (BER) increase, data rate loss, and computational complexity increase. These techniques include amplitude clipping, clipping and filtering, coding, tone reservation (TR), tone injection (TI), active constellation extension (ACE), and multiple signal representation techniques such as partial transmit sequence (PTS), selected mapping (SLM), and interleaving [5–8]. Above all, we would like to highlight the precoding technique since

✉ Nan Chi
nanchi@fudan.edu.cn

1 Beijing Institute of Technology, Beijing, China

2 Department of Communication Science and Engineering, State Key Lab of ASIC & System, Information School, Fudan University, No. 220, Handan Road, Yangpu District, Shanghai 200433, China

3 Science and Technology on Space Microwave Laboratory, China Academy of Space Technology, Beijing, China

it involves no nonlinear distortion to the original data and the computational complexity is comparatively low. Moreover, it has no limit on subcarriers' number and baseband modulation format. Recently, we have already experimentally demonstrated a novel 60 GHz RoF system with OFDM signals generated by precoding technique based on SQRC function [9]. However, none of PAPR reduction technique mentioned above has been introduced to VLC system to solve the PAPR issue of OFDM modulation.

In this paper, we propose the SQGNRC function and further improve the precoding matrix based on that. Considering the data redundancy introduced by precoding, there is a trade-off between PAPR improvement and sacrificed data bandwidth. Hence, the parameter optimization of the precoding matrix has also been discussed in detail. The proposed precoding matrix with optimized parameters can further reduce PAPR by nearly 1 dB compared with existing precoding matrix used in [9] and significantly achieve 3.5 dB PAPR reduction improvement in contrast to original OFDM signals. We have also experimentally verified the effect of the improved precoding matrix based on SQGNRC function in a VLC system employing phosphor-based white LED. To our knowledge, this is the first time precoding technique is utilized in VLC system to conquer the PAPR issue. The experimental results show that 140 cm transmission of precoded 32 quadrature amplitude modulation (QAM) OFDM signals at raw data rate of 1.35 Gbps can be successfully achieved below 7% forward error-correction (FEC) threshold of 3.8×10^{-3}. Furthermore, precoded signals significantly outperform original signals by BER performance of 1.62 dB at the same data bandwidth and 0.76 dB at the same raw data rate in terms of Q factor, which clearly demonstrates that the proposed precoding technique is promising in future VLC system.

2 Principle

Figure 1 shows the block diagram of precoding technique, including transmitter and receiver.

At the transmitter of the precoding technique, the input data is first modulated on baseband using QAM mapping. The baseband-modulated symbols are then grouped into different blocks of size $N \times 1$, which can be written as $X = \left[X_0, X_1, X_{2\ldots}X_{N-1}\right]^T$. Then, each block is precoded by a precoding matrix P of size $L \times N$. So the original symbol block X is transformed into precoded symbol block as $Y = PX = \left[Y_0, Y_1, Y_{2\ldots}Y_{L-1}\right]^T$, in which the precoded symbols can be written as $Y_m = \sum_{n=0}^{N-1} p_{m,n} X_n, m = 0, 1 \ldots L-1$. Finally, all precoded blocks are combined together and compose the actual transmitted OFDM symbol block:

$$x(t) = \sum_{m=0}^{L-1} Y_m e^{j2\pi m \frac{t}{T}}, \quad 0 \le t \le T \tag{1}$$

where T is the symbol period.

It is noted that $p_{m,n}$ is the element of precoding matrix which is waiting to be designed, $L = N + N_p$ is the actual total number of subcarriers and N_p is the redundant number of subcarriers. We define the portion of the extra subcarriers used by the precoder as the redundant factor, which is presented as $ratio = N_p/N = (L-N)/N$. When no coding is used, the matrix P reduces to an $N \times N$ identity matrix, and no redundant subcarrier is applied.

As illustrated in [6], assuming the average power of each symbol is equal, the PAPR of precoded OFDM signals at a given time interval [0, T) is directly related to N positive functions $|P_n(t)|$, which are determined by $p_{m,n}$:

$$\begin{aligned} PAPR &= \frac{\max |x(t)|^2}{E\left\{|x(t)|^2\right\}} \\ &= \frac{1}{L} \max_{0 \le t < T} \left(\sum_{n=0}^{N-1} \left| \sum_{m=0}^{L-1} p_{m,n} \exp\left(j2\pi m \frac{t}{T} \right) \right| \right)^2 \\ &= \frac{1}{L} \max_{0 \le t < T} \left(\sum_{n=0}^{N-1} |P_n(t)| \right)^2 \end{aligned} \tag{2}$$

Thus we define $P_n(t)$ as functions with cyclic shift within each other as (3) so as to avoid the peak amplitudes of the N functions $|P_n(t)|$ occurring at the same time instant. As a result, the PAPR will be reduced.

$$P_n(t) = \begin{cases} P_0(t - nT_s + T) & 0 \le t < nT_s \\ P_0(t - nT_s) & nT_s \le t < T \end{cases} \tag{3}$$

By letting $P_n(t)$ be the mother function of (3) and relate all the other functions to it, we get the following result:

$$P_n(t) = \sum_{m=0}^{L-1} p_{m,0} e^{-j2\pi \frac{mn}{L}} e^{j2\pi m \frac{t}{T}} \tag{4}$$

illustrating that entries from the columns other than the first column are decided by the entry of the first column as follows:

$$p_{m,n} = p_{m,0} e^{-j2\pi \frac{mn}{L}} \tag{5}$$

In [6], we selected SQRC function as the precoding function to determine the first column of the precoding matrix and thus get the whole matrix based on (4). To further achieve better PAPR reduction performance, we consider improving the precoding matrix based on new precoding function. We noticed that [10] has proposed generalized raised cosine (GNRC) function which is defined as:

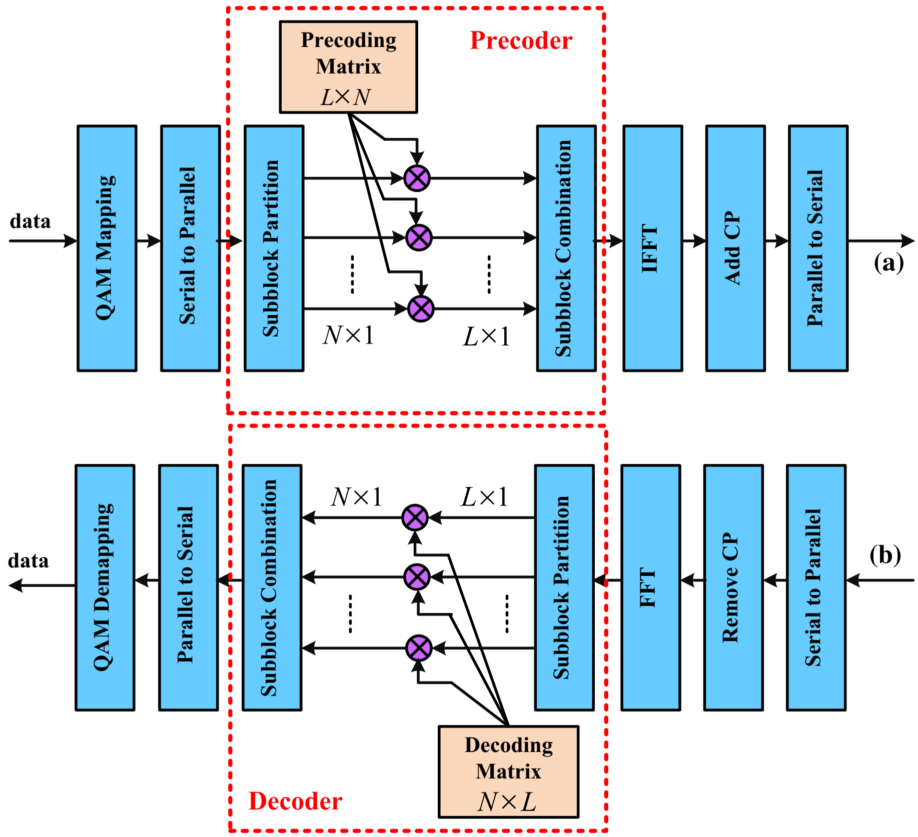

Fig. 1 Block diagrams of precoding technique. **a** Transmitter. **b** Receiver

$$H_{GNRC}(f) = \frac{T}{2}\left\{1 + \frac{2}{\alpha}(1 - 2T|f|) - q\cos\left[\frac{\pi T}{\alpha d}\left(|f| - \frac{(1-\alpha d)}{2T}\right)\right]\right\}, \quad \frac{1-\alpha}{2T} < |f| \le \frac{1+\alpha}{2T} \tag{6}$$

where α is the roll-off factor and d is the shaping factor which is introduced to generalized the conventional raised cosine (RC) function by allowing multiple or fraction of one half-cycle of cosine to be fitted in the transition region $\frac{1-\alpha}{2T} < |f| \le \frac{1+\alpha}{2T}$. Besides, $q = \cos^{-1}(\frac{\pi}{2}\frac{(d-1)}{d})$ is the amplitude normalization factor to ensure continuous frequency responses across the borders between different regions.

Based on the definition of GNRC function above, we further propose the definition of SQGNRC function as illustrated in (7) and select it as the improved precoding function to determine first column of the proposed precoding matrix as shown in (8).

$$H_{SQGNRC}(f) = \frac{T}{2}\sqrt{\left\{1 + \frac{2}{\alpha}(1 - 2T|f|) - q\cos\left[\frac{\pi T}{\alpha d}\left(|f| - \frac{(1-\alpha d)}{2T}\right)\right]\right\}}, \quad \frac{1-\alpha}{2T} < |f| \le \frac{1+\alpha}{2T} \tag{7}$$

$$p_{m,0} = \begin{cases} \frac{(-1)^m}{\sqrt{N}}\sqrt{\left\{\frac{4m}{N_p} - 1 - q\cos\left[\frac{\pi}{d}\left(\frac{m}{N_p} - \frac{1+d}{2}\right)\right]\right\}}, & 0 \le m \le N_p \\ \frac{(-1)^m}{\sqrt{N}} & N_p < m \le N \\ \frac{(-1)^m}{\sqrt{N}}\sqrt{\left\{3 + \frac{4}{\alpha} - \frac{4m}{N_p} - q\cos\left[\frac{\pi}{d}\left(\frac{m}{N_p} + \frac{d-1}{2} - \frac{1}{\alpha}\right)\right]\right\}}, & N < m \le L-1 \end{cases} \tag{8}$$

Here, we have $\alpha = ratio = \frac{N_p}{N} = \frac{L-N}{N}$ and $q = \cos^{-1}(\frac{\pi}{2}\frac{(d-1)}{d})$. It is obvious that the proposed precoding matrix directly depends on two parameters: the redundant factor: *ratio* and shaping factor: d. The optimization of the parameters mentioned above will be discussed in detail in the following part.

As shown in Fig. 1b, at the receiver the decoding is performed to recover the OFDM symbol block. The decoding matrix is the inverse matrix of the precoding matrix which is used to cancel out the influence of precoding on the actual transmitted data.

The PAPR reduction performance of the proposed precoding matrix is further measured by the complementary cumulative distribution function (CCDF), which is defined as the probability of PAPR exceeding the threshold *PAPR0*:

$$CCDF = P(PAPR > PAPR0) \quad (9)$$

In the following, Figs. 2 and 3 present series of simulation results. Figure 2 shows the influence of parameters (*ratio* and d) on the threshold *PAPR0* when CCDF is fixed at 10^{-2}. We limit the redundant factor *ratio* within 5–50% and adjust shaping factor d from 0 to 2.5. As highlighted by circle 1, there exists an ideal region for *ratio* and d in which the threshold *PAPR0* can reach the minimum value of 5.5 dB, and thus we will achieve the best PAPR reduction performance.

However, within such ideal regions, the redundant factor *ratio* is quite high (> 25%). Actually, when *ratio* is set at 10%, the threshold *PAPR0* can already reach 6.5 dB if d is selected within the appropriate range, just as labeled by circle 2. Considering the improved effect of increasing *ratio* from 10 to 25% is comparatively limited, we conclude that *ratio* at 10% keeps a wise trade-off between PAPR reduction and the scarification of data bandwidth. Based on this premise, we set d at 1.075 to obtain the minimal value of *PAPR0*.

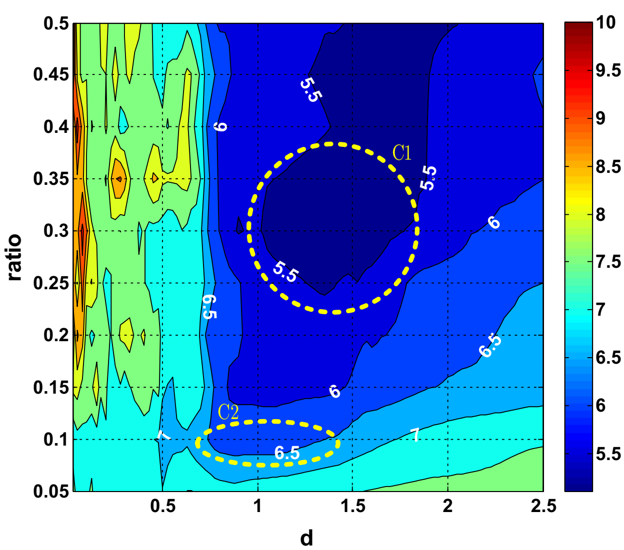

Fig. 2 Influence of ratio and d on threshold PAPR0 when CCDF = 10^{-2}

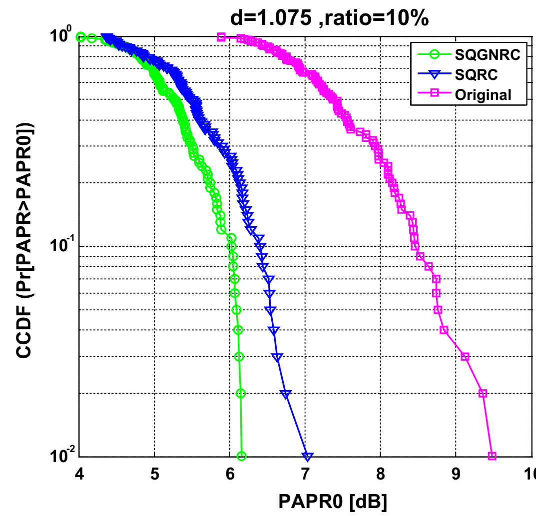

Fig. 3 CCDF of original OFDM signals and precoded signals based on SQGNRC/SQRC function

At the optimum value of *ratio* and d, the CCDF curves of original OFDM signals without precoding, precoded OFDM signals generated by existing SQRC precoding matrix and proposed SQGNRC precoding matrix are shown in Fig. 3. As expected, the precoded OFDM signals based on proposed SQGNRC precoding matrix have lower PAPR probability than that of other two cases. In particular, when compared with original OFDM signals without precoding, the PAPR can be significantly reduced by nearly 3.5 dB at CCDF = 10^{-2} when the sacrificed data bandwidth is well controlled at 10%. Moreover, when compared with the existing SQRC precoding matrix, PAPR can be further reduced by 1 dB through the proposed SQGNRC precoding matrix.

3 Experimental setup and results

Figure 4a presents the experimental setup for the proposed VLC system utilizing phosphor-based white LED.

At the transmitter, the input bit sequence is first segmented into blocks and mapped into complex symbol of 32QAM. Precoding based on proposed SQGNRC function is performed to original symbol blocks before inverse fast Fourier transform (IFFT). After adding cyclic prefix, complex-to-real-value conversion is achieved by up-conversion. The total number of used subcarriers L is 256. The length of the cyclic prefix is 1/16 of the symbol period. Finally, the offline generated precoded 32QAM OFDM signal is uploaded into an arbitrary wavelength generator (AWG, Tektronix 710). Then the output signal from AWG is equalized by a self-designed

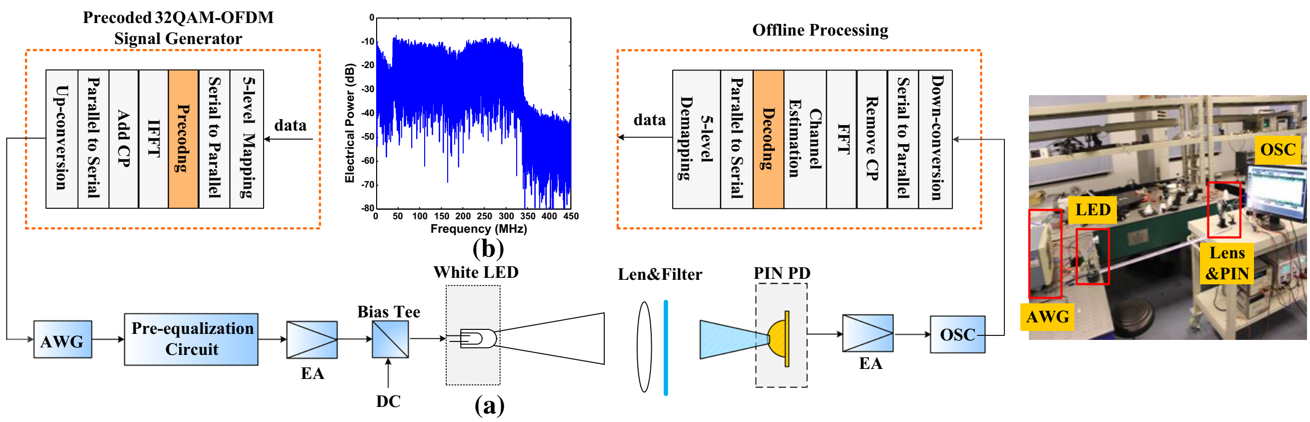

Fig. 4 **a** Experimental setup for the proposed VLC system utilizing phosphor-based white LED **b** Electrical spectrum of the received precoded 32QAM OFDM signal, *AWG* arbitrary wavelength generator, *EA* electrical amplifiers, *DC* direct current, *PIN PD* PIN photodiode, *OSC* oscilloscope

bridged-T pre-equalization circuit [11] to compensate the frequency attenuation of LED at high frequencies. After amplified by electrical amplifiers (EA), the resulting signal coupled with DC-bias voltage by a bias tee is applied to the phosphor-based white LED as the transmitter. After $\geq$ 100 cm free space delivery, the modulated light is focused onto the PIN photodiode (PIN PD, Hamamatsu 10784) through a focusing lens. In front of the PIN PD, a blue filter which compresses the phosphorescent component is implemented. Then, the detected electrical 32QAM OFDM signals pass through an EA and are sampled by a real-time digital oscilloscope (OSC, Agilent 54855A). The sampled electrical signals are differential detected at first and down-converted for further offline processing, including OFDM demodulation, decoding and 32QAM de-mapping. Post-equalization based on training symbols is used for compensation of the channel impairments. The measured electrical spectrum of the received precoded 32QAM OFDM signal is presented in Fig. 4b as well.

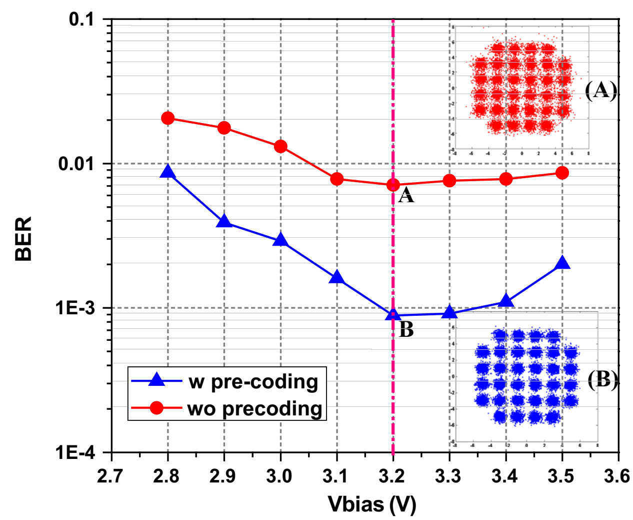

Fig. 5 BER versus bias voltage of precoded/original signals

4 Results and discussion

At first, the influence of different bias voltages is investigated to ensure the LED works at the optimal condition. We measure the BER performance versus phosphor-based white LED's bias voltages both in the case of precoding and without precoding. According to the results shown in Fig. 5, the optimal bias voltages of the phosphor-based white LED for both cases are the same, which should be set at 3.2 V.

On this basis, we further optimize signal drive voltage *Vpp* for the phosphor-based white LED both for the precoding and original signals. As shown in Fig. 6, when the bias voltage is fixed at 3.2 V for both cases, the optimal *Vpp* for precoded signals is 1.2 V which is 0.2 V smaller than that of original signals. This is mainly because amplitude normalization is conducted at the transmitter; thus, the effective amplitude range of precoded signals with lower PAPR will be larger than that of original signals under the same *Vpp*. To eliminate the influence of normalization, larger *Vpp* is needed for original signals.

The BER performance versus transmission distances with and without precoding is measured and presented in Fig. 7. Due to the expense of 10% redundant subcarriers, the raw data rate of precoded 32QAM OFDM signals at 300 MHz bandwidth is 1.35Gbps. Therefore, we evaluate the performance of original signals at the same bandwidth and raw data rate, respectively. The Q factor for each case is also marked in Fig. 7 for reference. As shown in Fig. 7, by utilizing the precoding technique based on SQGNRC function, 140 cm transmission of 1.35 Gbps 32QAM signals can be successfully achieved below pre-FEC limit of 3.8×10^{-3}. When the distance is fixed at 125 cm, precoded 32QAM OFDM signals obviously outperform original signals by BER performance of 1.62 dB at the same bandwidth and 0.76 dB at the same

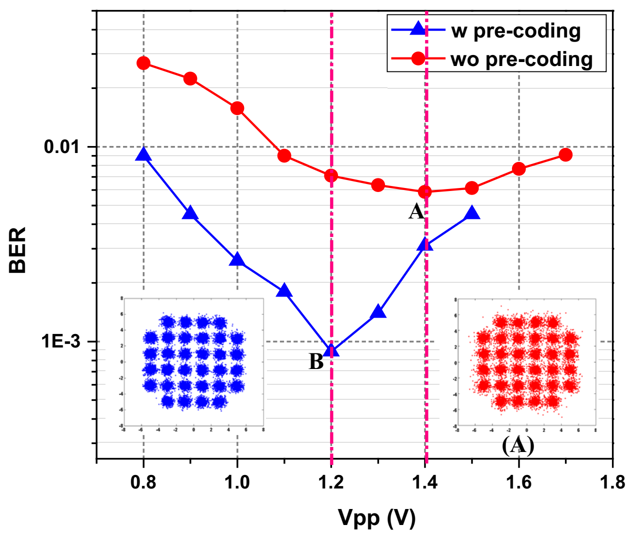

Fig. 6 BER versus signal drive voltage Vpp of precoded/original signals

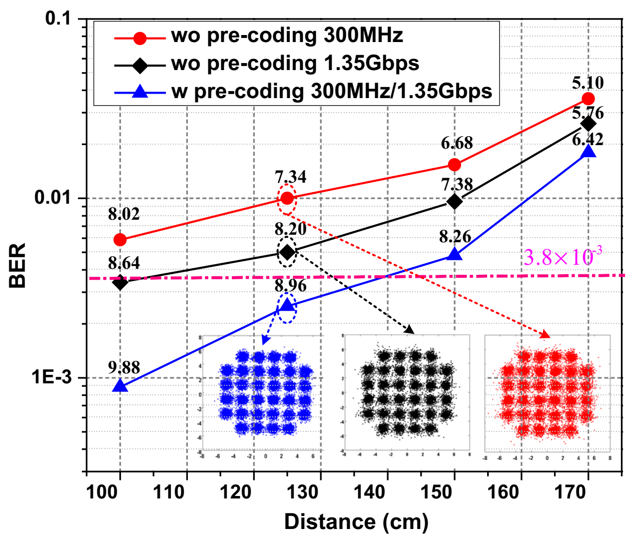

Fig. 7 BER versus transmission distance of precoded/original signals

raw data rate in terms of Q factor. The corresponding constellations for each case are also inserted for comparison. Furthermore, the luminance after the focusing lens, another key factor relating to the transmission distance in VLC system, is also measured and given as follows: 100 cm 120 lx, 125 cm 96 lx, 150 cm 72 lx, and 170 cm 51 lx, which are all below the standard value for brightness (500 lx). It is believed that distance can further improved by increasing the optical power of LEDs or deploying a LED array.

5 Conclusions

A novel precoding matrix based on SQGNRC function for PAPR control is proposed and experimentally verified through a VLC system utilizing phosphor-based white LED in this paper. To our knowledge, this is the first time precoding technique is utilized in VLC system to conquer the PAPR issue. The simulation results show that the proposed precoding matrix can achieve 3.5 dB improvement in contrast to original signals without precoding at CCDF $= 10^{-2}$. Moreover, the experimental results show that 140 cm transmission of precoded 32QAM signals at raw data rate of 1.35 Gbps can be successfully achieved below 7% FEC threshold of 3.8×10^{-3}. Finally, precoded signals effectively outperform original signals by Q factor of 1.62 dB at the same bandwidth and 0.76 dB at the same raw data rate, which clearly demonstrates the benefit and feasibility of proposed precoding technique in future VLC system.

Acknowledgements This work was partially supported by the NSFC project (No. 61571133), and Key project of Guangdong province (2014B010119003).

References

[1] Wang, Y., Wang, Y., Chi, N.: Experimental verification of performance improvement for a gigabit wavelength division multiplexing visible light communication system utilizing asymmetrically clipped optical orthogonal frequency division multiplexing. Photon. Res. **2**(5), 138–142 (2014)

[2] Shao, Y., Chi, N., Fan, J., et al.: Generation of 16-QAM-OFDM signals using selected mapping method and its application in optical millimeter-wave access system. IEEE Photon. Technol. Lett. **24**(15), 1301–1303 (2012)

[3] Chen, X., Li, A., Gao, G., et al.: Experimental demonstration of improved fiber nonlinearity tolerance for unique-word DFT-spread OFDM systems. Opt. Express. **19**(27), 26198–26207 (2011)

[4] Wunder, G., Fischer, R.F.H., Boche, H., et al.: The PAPR problem in OFDM transmission: New directions for a long-lasting problem[J]. arXiv preprint arXiv:1212.2865, (2012)

[5] Han, S.H., Lee, J.H.: An overview of peak-to-average power ratio reduction techniques for multicarrier transmission. IEEE. Wirel. Commun. **12**(2), 56–65 (2005)

[6] Armstrong, J.: Peak-to-average power reduction for OFDM by repeated clipping and frequency domain filtering. Electron. Lett. **38**(5), 246–247 (2002)

[7] Shao, Y., Wang, Y., Chi, N.: 60-GHz RoF system with low PAPR 16QAM-OFDM downlink using PTS segmentation. IEEE Photon. Technol. Lett. **25**(9), 855–858 (2013)

[8] Davis, J.A., Jedwab, J.: Peak-to-mean power control in OFDM, Golay complementary sequences, and Reed-Muller codes. IEEE Trans. Inf. Theory **45**(7), 2397–2417 (1999)

[9] Wang, Y., Li, X., Tao, L., et al.: A novel PAPR reduction algorithm based on precoding techniques applied in 60GHz OFDM-RoF system. In: Asia Communications and Photonics Conference. Optical Society of America, p. ATh3G.2 (2013)

[10] Rha, Peter S., Hsu, Sage: Peak-to-average ratio (PAR) reduction by pulse shaping using a new family of generalized raised cosine filters. IEEE. Veh. Technol. Conf. **1**, 706–710 (2003)
[11] Huang, X., Shi, J., Li, J., et al.: 750 Mbit/s visible light communications employing 64QAM-OFDM based on amplitude equalization circuit. Accepted by Optical Fiber Communication Conference (OFC), Tu2G.1 (2015)

Hai-Chao Guo received the B.S. degree in optical Engineering from University of Electronic Science and Technology in 2006 and M.S in Electrical Engineering from University of Chinese Academy of Sciences in 2009, respectively. During 2009-, he studies satellite free space coherent optical communication and laser imaging in National key Lab. Of Science and Technology on Space Microwave and Beijing Institute of Technology School of Information and Electronics.

Yin-Fan Xu studies visible light communication technology in Fudan University from July 2014 and will receive the bachelor degree in Communication Science and Engineering from Fudan University in June 2017. She received the B.S. degree in communication engineering from Wuhan University of Technology in 2014.

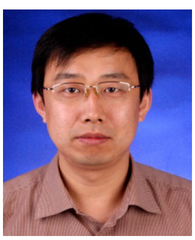

Xiao-Jun Li a space communication advanced engineer, received the Ph.D.in information and signal processing from Xidian University, Xi'an, China, in 2004. Currently, he is the deputy director of the National Key Lab of Science and Technology on Space Microwave. Besides, he is also the director of Shannxi Image and Graphics Society. He is mainly research on the space satellite communication technology, image processing technology and smart intelligence information processing technology and so on. At the present time, he has authored or coauthored over 10 patents in China and over 30 technical publications in refereed journals and conferences proceedings.

Li Zhang received the B.S. degree and M.S in thermal analysis from Xi'an Jiaotong University in 2006 and 2009, respectively. During 2009-, she studies satellite thermal design drawing analysis in China Academy of Space Technology Xi'an.

Yan-Jin Wang received the bachelor degree in Communication Science and Engineering from Fudan University in 2012 and master degree in Optical Communication from Fudan University in 2015. During the study in Key Laboratory for Information Science of Electromagnetic Waves (MoE), her research interests mainly cover Radio over Fiber technology and coherent optical communication system.

Nan Chi received the B.S. degree and Ph.D. degree in electrical engineering from Beijing University of Posts andTelecommunications, Beijing, China in 1996 and 2001, respectively. From July 2001 to December 2004, she worked as assistant professor at the Research Center COM, Technical University of Denmark, Lyngby, Denmark. From January 2005 to April 2006, she was a research associate at the University of Bristol, Bristol, United Kingdom. She joined Wuhan National Laboratory for Optoelectronics, Huazhong University of Science and Technology from June 2006 to May 2008, where she worked as a full professor. Since May 2008, she joined Fudan University. She is the author or co-author of more than 100 papers. Her research interests are in the area of convergence of wireless and optical network, all-optical processing and advanced modulation formats.